The Value of 18F-Fluorodeoxyglucose PET (18F-FDG PET) and MRI Spectroscopy in Underpinning Suspicious Breast Cancer

Shazreen, S.[1]*, Shakher, R.[2], Shahrun Niza, A. S.[3] and Fathinul Fikri, A. S.[1]

[1]Departmentof Diagnostic and Nuclear Imaging, University Putra Malaysia, 43400 UPM, Serdang, Selangor, Malaysia
[2]Department of Nuclear Imaging, Monash University, Clayton VIC 3800, Australia
[3]Department of Surgical, Universiti Kebangsaan Malaysia, 43600 UKM, Bangi, Selangor, Malaysia

ABSTRACT

The aim of this study was to evaluate the value of MRI spectroscopy and association with the altered glucose metabolism on 18-FDG PET/CT in patients with suspicious breast cancer. Eight selected breast cancer patients with BIRADS 4 or 5 on mammogram were recruited and patients underwent 18F-FDG PET/CT MRI (spectroscopy). The standardise uptake value (SUVmax) was analysed to determine the degree of the altered glucose metabolism on the PET. The metabolites of tumor lesions were measured using *in vivo* proton MR spectroscopy (MRS) of the breast. There were eight females with a mean age of 55.3±12.2 years with a biopsy result of invasive ductal carcinoma (2), lobular carcinoma (1) and benign lesion (5). There was a significant difference between the mean of the malignant tumour (SUVmax 4.28±3.74 g/ml) and the mean of the benign tumour (SUVmax: 2.33±0.9 g/ml). On the per-lesional basis of the MRS correlate with SUVmax, the suspicious breast tissue exhibited raised creatinine metabolites (mean: 3.39±0.54u) with significant correlation SUVmax mean 3.06±2.34 as compared to N-acetyl Aspartate (NAA), (mean: 2.84±0.99u) and choline (mean: 2.46± 0.70 u). This study showed that high SUVmax was associated with malignant cancer and the high creatinine metabolite that correlated with the SUVmax could potentially be utilised as a surrogate marker in detecting breast cancer.

Keywords: Magnetic Resonances Imaging Spectroscopy, Computed tomography, positron emission tomography, [18F]-fluorodeoxyglucose, multimodality

INTRODUCTION

Worldwide, breast cancer is becoming a leading cause of death. Mortality due to breast cancer increased from 20,100 deaths in 2008 to 21,700 deaths in 2012 worldwide, as reported by the International Agency for Research on Cancer (IACR) Globocan of the

World Health Organisation (WHO). The risk factors that contribute to breast cancer include hormone replacement therapy for a long period of time, being overweight especially after menopause and mutations in cancer-related genes (erbB2). Recent studies found that the development of cancer was due to choline intake (Zhang et al., 2013).

In breast cancer cells, the level of choline was found markedly higher compared to in normal human mammary epithelial cells (Aoyama et al., 2004). Both choline phosphorylation and transport were found to be augmented in human breast cancer cells (Cho et al., 2007). Overexpression of choline kinase (CK) will induce progression of human mammary epithelial cells from a normal to a malignant phenotype. These choline kinase will catalyse the phosphorylation of choline to form phosphocholine, followed by generation of phosphatidylcholine in tumor cell membranes (Molina et al., 2004). Recent studies proved that choline kinase, which transforms choline to phosphocholine (PCho), was increased in malignant tumours and caused progression of mammary epithelial cells *in vitro* (Ramirez et al., 2004).

In vivo proton MR spectroscopy (^{1}H-MRS) is a non-invasive technique that has great potential to generate tumor metabolism, which is a useful process in evaluation and diagnosis of the response to treatment of tumour progression (Meisamy et al., 2004). Recently, breast ^{1}H-MRS has been shown to improve cancer diagnosis based on elevated choline-containing compounds' (tCho) metabolite peak (Baek et al., 2008). Several researchers have found that 1.5T of *in vivo* ^{1}H-MRS can be used to detect and distinguish between malignant and benign cancer tissue (Baik et al., 2006). Nowadays, FDG ia used to detect tumour progression by providing useful information about tumor characterisation, staging, patient prognosis and monitor response of anticancer therapy to patients with suspected malignancies. Besides that, FDG uptake correlates with tumour growth and viability in recent studies (Fathinul Fikri et al., 2014). A combination of non-invasive imaging techniques of Positron Emission Tomography (PET) and MRI are beneficial in detecting the response to treatment to target tumours using the metabolics of choline. The aim of this study was to evaluate the value of metabolic MRI spectroscopy and its association with altered glucose metabolism on FDG-18 PET/CT in patients suspected of developing breast cancer tissue as evaluated by the BIRADS scoring system.

MATERIALS AND METHODS

Patient Selection

In the prospective group, eight selected breast cancer patients with mammogram results showed BIRADS 4 or 5, recurrent breast cancer and biopsy results with proven breast mass were recruited from an endocrinology clinic. Patients undergoing chemotherapy or who had undergone surgery were excluded from the studies. All the patients underwent 18F-FDG PET CT and MRI spectroscopy prospectively. All the patients who participated in this study gave written consent before commencement of the study.

Patient preparation. All the patients were required to fast from food consumption for at least 6 hr before examination. The fasting blood glucose level was measured in the morning and followed by injection of the tracer of 8-10mCi of ^{18}F-FDG intravenously. The patients

were required to rest with an uptake time approximately 60 min in a confinement room before examination. All the patients underwent MRI imaging first, followed by PET-CT imaging studies according to standard protocol.

Imaging Technique

^{18}F-FDG. The dedicated integrated PET-CT system (Siemens Biograph-64, Germany) was used to standardise the value of ^{18}F-FDG uptake. This dedicated PET scanner with optimum performance in 3-D Imaging using Lutetium Oxyyorthosilicate (LSO) scintillator crystal technology was used to provide efficient rejection of random events, fast coincidence timing, high count rates and high light output. The device was incorporated with a multislice CT scanner with capability for high spatial resolution and a 64-slice CT. For higher sensitivity, the acquisition time for PET using this system was calibrated using a 2-min-per-table position. The CT data were resized from a 512x512 matrix to a smaller matrix, 128x128, to match the PET data to allow the fusion image and CT transmission map to be generated. Ordered-subsets expected maximisation (OSEM) was used to reconstruct the PET images with segmented measurement of attenuation correction using CT data with four iterations and 16 subsets. Post reconstruction smoothing of images was performed using a 5-mm FWHM Gaussion filter. The PET and CT images were then fused, creating an image of distributed ^{18}F-FDG overlying the corresponding anatomy and physiology generated using a dedicated workstation.

MRI spectroscopy. MRI was performed using a 3.0-T system (Prisma, Siemens Heatlcare). All patients were examined in a prone position. A bosy coil was used for transmission and a double-breast coil (4-element Breast Matrix Coil, Siemens Helathcare) was used for the MR spectroscopy. All the MRI sequence steps were performed using a single-voxel ^{1}H MRS with a point-resolved spectroscopy sequence (PRESS). The parameter of MRS was 1,620/270;voxel size 10x10x10 mm^3; 256 acquisitions; spectral width 1000Hz; 1,024 data points; and the time of acquisition, 7 min. For voxel placement, coronal and sagittal positions were used as scout images, and a voxel of interest was placed to include the lesion. Shimming was performed automatically first, followed by manual shimming on the water resonance for optimisation of the homogeneity in each volume of interest. Water-peak line widths of 10-20Hz (full width at half-maximum [FWHMI]) were typically achieved. After the shimming procedure, spectra were acquired with water suppression by applying three chemical shift-selective excitation pulses. By spectral suppression using dual band-selective inversion with gradient dephasing, the transverse magnetisation was selectively dephased before and after the second spin-echo pulse.

Image Analysis

The PET/CT scans and MRI breast images were read and interpreted by an experienced radiologist with more than five years' clinical experience, who was blinded to the history and diagnosis of each patient and was unaware of any clinical findings or information.

^{18}F-FDG. The results were analysed according to the qualitative assessment on a per-lesion basis in each patient who had undergone the FDG-PET/CT examination. On per lesion basis,

the higher inherent metabolic activity was compared to the mediastinal blood pool on the FDG-PET/CT and the lesions were considered positive lesions. All of the reviews of the PET images and the determination of the PET parameter were performed via software using a setting that allowed maximum intensity projection (MIP) and three-dimensional displays (transaxial, coronal, sagittal) of PET, CT and fused PET/CT images. The SUVmax was derived from the mean of all the FDG-positive lesions. The CT scans were also analysed for lesion location, size and the pattern of regional tumour infiltration. For the quantitative assessment, a circular region of interest (diameter 1.5 cm) was placed over the tumour in the slice with the maximum SUV in the baseline scan (Figure 1).
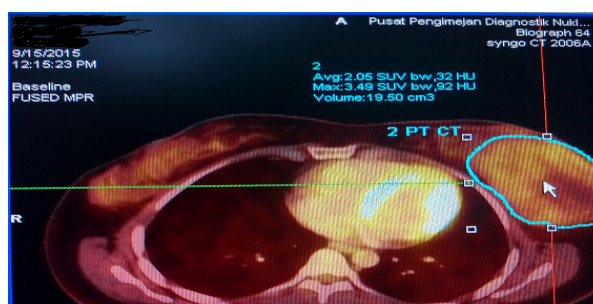

Figure 1. A circular region of interest (diameter 1.5 cm) was placed over the tumour in the slice with the maximum SUV of 3.49ug/dl

MRI spectroscopy. The obtained spectrum represents specific metabolites appearing in certain frequencies due to their specific chemical shifts. The resonance spectrum identifies metabolites by locating their peaks. Several peaks can characterise the same compound (i.e. doublet or triplet). Graphic representation of acquired data includes these metabolite peaks (represented on the horizontal axis of the graph) expressed as parts per million (ppm) and their relative signal amplitude in the vertical axis. The area or integral under each peak represents the relative concentration of the detected metabolite (Figure 2).
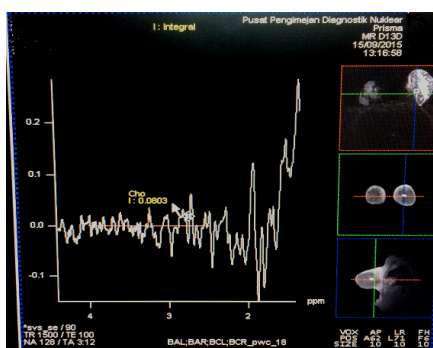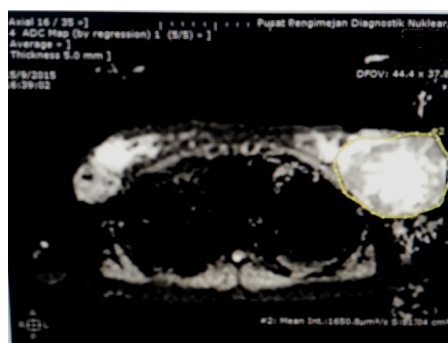
a   b

Figure 2. (a) The peak of tCho with 1.41 ppm, integral at 0.08 in benign tumour. (b) The circular region drawn at the breast lesion with *b* value of 50 showed non-restricted ADC value of $1.65 mm^2/s$, which was benign

Statistical Analysis

All the patients with biopsy-proven cancer were dichotomised into groups based on malignant and benign cancer. Univariate descriptive analysis was carried out using socio-demographic characteristics (age group and biopsy results). Numerical data described using means and standard deviation depending on the distribution of respective variables (Table 2). An independent t test was used to compare between the groups (Table 3). Data were analysed using the Pearson correlation coefficient. All statistics were analysed using the Statistical Package for Social Sciences programme for Windows 21.0 (SPSS 21) (IBM Corp, Somers, New York). P values <0.05 were considered statistically significant.

Table 1
Descriptive patient characteristics (n=8)

Characteristic	N (n=8)	Percentage
Age Group (Years)		
<30	1	12.5
31-40	5	62.5
41-50	2	25
Biopsy		
Fibroadenamatous	3	37.5
PASH	1	12.5
Fibroadenosis	1	12.5
IDC	2	25
ILC	1	12.5

RESULTS AND DISCUSSION

Patient Characteristics

The mean age of the patients in our study was 55.3±12.2 years, with middle age of 31-40 years being predominant (62.5%). Most of the subjects showed BIRADS 4 majority. The biopsy results showed five benign patients with three fibroadenoma, one Pseudoangiomatous Stromal Hyperplasia (PASH) and one fibroadenosis, while three patients showed malignant tumours with two Invasive Ductal Carcinoma (IDC) and one Invasive Lobular Carcinoma (ILC) (Table 1).

The relationship between biopsy with SUVmax and parameter of MRI spectroscopy. Table 2 shows there was significant relationship between SUVmax ($p<0.05$) and the biopsy results; the mean for malignant tumours was 4.28±3.74 and the mean for benign tumours was 2.33±0.90, while there was no significant correlation between the biopsy results and the MRI parameters.

Table 2

Relationship between biopsy with FDG uptake (SUVmax) and MRI spectrocopy using independent t test

	Biopsy	*n*	Mean	Std. Deviation	*p* value
FDG (SUVmax)	malignant	3	4.28	3.74	*0.01
	benign	5	2.33	0.90	
MRI spectroscopy choline	malignant	3	3.25	0.14	0.4
	benign	5	2.00	0.34	
MRI spectroscopy creatinine	malignant	3	3.45	0.70	0.44
	benign	5	3.39	0.52	
MRI spectroscopy N-acetyl Aspartate (NAA)	malignant	3	2.77	1.29	0.42
	benign	5	2.88	0.93	

*statistical significance p<0.05

Correlation between SUVmax and parameter of MRI spectroscopy. There was significant and direct correlation between FDG uptake with a mean of 3.06±2.34 and the creatinine mean of 3.39±0.54, where p=0.02. Besides that, there was also a significant and direct correlation between the FDG uptake with a mean of 3.06±2.34 and the N-acetyl Aspartate (NAA) mean of 2.84±0.99, where p=0.05 (Table 3).

Table 3

The correlation between FDG uptake (SUVmax) and parameter of MRI spectroscopy using Pearson correlation

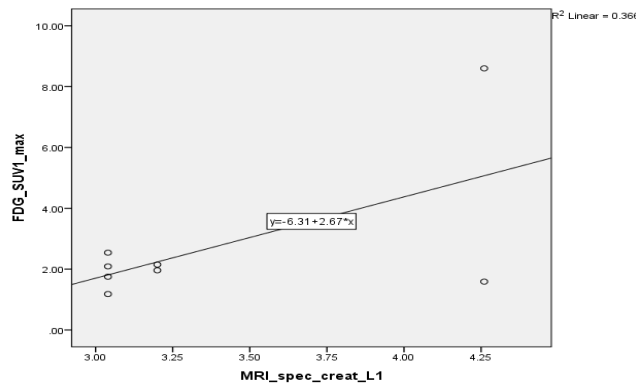| SUVmax vs MRI spectroscopy	mean±S.D	r value	p value
-FDG (SUVmax)	3.06±2.34	0.16	0.32
-MRI spectroscopy choline	2.46±0.7		
-FDG (SUVmax)	3.06±2.34	0.63	*0.02
-MRI spectroscopy creatinine	3.39±0.54		
-FDG (SUVmax)	3.06±2.34	0.5	*0.05
-MRI spectroscopy NAA	2.84±0.99		

* statistical significance p<0.05

Figure 3. Scatter plot correlating the relationship between SUVmax and creatinine using Pearson correlation test

The level of choline in the human breast cancer cells was found to be markedly higher than in normal human mammary epithelial cells (Aoyama et al., 2004). Both choline transport and phosphorylation were found to be augmented in the human breast cancer cells. Progression of human mammary epithelial cells from normal to malignant phenotype was shown to be associated with an induced overexpression of choline kinase (CK) that catalysed the phosphorylation of choline to form phosphocholine followed by generation of phosphatidylcholine in the tumour cell membranes (Molina et al., 2004). In previous studies, the increased choline uptake in tumour cells was mainly explained by the upregulation of choline kinase due to an increased demand of membrane constituents (Molina et al., 2004). Recent studies found that the development of cancer was due to choline intake (Zhang et al., 2013). Besides that, other studies have proven that CK and phosphorylcholine (PCho) production increased in growth factor-induced mitogenic signaling of primary human breast epithelial cells in response to insulin and hydrocortisone (Ramirez et al., 2004).

Imaging of tumour cell metabolism has been remarkably successful in recent years. Numerous studies have demonstrated that malignant tumours can be detected with high sensitivity and specificity by imaging increased metabolic rates for glucose. FDG Positron Emission Tomography (PET) has been extensively used as an imaging biomarker for diagnosis (Kelloff et al., 2005) and for monitoring of treatment response in cancer patients. An accumulation of the radiotracer-marked glucose, in terms of 18f-fluorodeoxyglucose, indicates an increased metabolic activity of viable tumour cells that can be quantified by SUV measurements. Our studies showed that there was a significant and increased FDG uptake in malignant lesions with a mean of 4.28 ± 3.74 compared to in benign lesions with a mean of 2.33 ± 0.90. This study showed that a high SUVmax was associated with malignant cancer.

In the mammary gland area, total choline, tCho or Cho, is considered the most important metabolite in proton MR spectroscopy. It has been reported that the degree of elevated choline-containing compounds is related to the grade of the tumour, with higher levels in high-grade than in low-grade lesions (Baik et al., 2006). Malignant lesions are more likely to show high levels of choline-containing compounds compared to benign or normal breast tissues. In this preliminary study utilising the 3.0T MR revealed that there was insignificant relationship

between biopsy results with and without choline. The mean tCho for malignant lesions is 2.58±1.01u compared to benign lesions, with a mean of 2.39±0.82u (p>0.05). Confounding factors i.e. patient motion, contamination by hemorrhage and inclusion of lipids interspersed with stromal and inflammatory cells may affect a small preliminary sample and would not yield a significant statistical results. The 3.0 Tesla MRI can unveil new potential surrogate molecular markers for aggressive lesions.

The Positron Emission Tomography (PET) and MR methods are two clinically translatable, non-invasive imaging techniques that are increasingly being used to detect physiological changes and the response of tumors to target therapy. Based on our study, we may conclude that there is direct and significant correlation between SUVmax 3.06±2.34g/dl and the parameter of MRI spectroscopy i.e. creatinine 3.39±0.54u and N-acetyl Aspartate (NAA). The metabolite landscape pattern showed that the highest mean was creatinine followed by N-acetyl Aspartate (NAA), (mean: 2.84±0.99u) and choline (mean: 2.46±0.70u).

The limitation of this study was its small sample size and high number of benign cases that made it difficult to generalise the results to the general population. Besides that, small and non-palpable lesions bonded to a small volume of the samples, and these were below the PET resolutions. Future studies are recommended to used large sample sizes with various histologic prognostic parameters such as nuclear grade and estrogen receptor status that can correlate with PET/CT and MRI spectroscopy in detecting primary breast cancer.

CONCLUSION

This study showed that high SUVmax associated with malignant cancer and high creatinine metabolites that correlate with SUVmax could potentially be utilised as surrogate markers for suspicious lesions in detecting breast cancer lesion suspected during mammography. Thus, a combination PET/CT and MR spectroscopy can be used to classify breast lesion as indicating stability or progressive disease with potential therapeutic relevance in underpinning breast cancer.

ACKNOWLEDGEMENT

REFERENCES

Aoyama, C., Liao, H., & Ishidate, K. (2004). Structure and function of choline kinase isoforms in mammalian cells. *Program Lipid in Research, 43*(3), 266–281.

Baek, H. M., Hon, J. Y., Chen, J. H., Nalcioglu, O., & Su, M. Y. (2008). Quantitative correlation between 1H MRS and dynamic contrast-enhanced MRI of human breast cancer. *Magnetic Resonance Imaging, 26*(4), 523–531.

Baik, H. M., Su, M. Y., Yu, H., Mehta, R., & Nalcioglu, O. (2006). Quantification of choline-containing compounds in malignant breast tumors by 1H MR spectroscopy using water as an internal reference at 1.5 T. *MAGMA, 19*(2), 96–104.

Burtscher, I. M., Skagerberg, G., Geijer, B., Englund, E., Stahlberg, F., & Holtas, S. (2000). Proton MR spectroscopy and preoperative diagnostic accuracy: An evaluation of intracranial mass lesions characterized by stereotactic biopsy findings. *American Journal of Neuroradiology, 21*(1), 84–93.

Chiuve, S. E., Giovannucci, E. L., Hankinson, S. E., Zeisel, S. H., Dougherty, L. W., Willett, W. C., & Rimm, E. B. (2007). The association between betaine and choline intakes and the plasma concentrations of homocysteine in women. *American Journal of Clinical Nutrition, 86*(4), 1073–1081.

Cho, E., Willett, W. C., Colditz, G. A., Fuchs, C. S., Wu, K., Chan, A. T. … Giovannucci, E. L. (2007). Dietary choline and betaine and the risk of distal colorectal adenoma in women. *Journal of the National Cancer Institute, 99*(16), 1224–1231.

Eberl, M. M., Fox, C. H., Edge, S. B., Carter, C. A. & Mahoney, M. C. (2006). BI-RADS classification for management of abnormal mammograms. *Journal of the American Board of Family Medicine, 19*(2), 161–164.

Fathinul Fikri, A. S., Abdul Jalil, N., & Lau, E. F. (2014). 18[F] FDG-PET/CT is a useful molecular marker in evaluating tumour aggressiveness; a revised understanding of an in-vivo FDGPET imaging that alludes the alteration of cancer biology. *Cell Biochemistry and Biophysic, 55*(5), 631–640.

Kelloff, G. J., Hoffman, J. M., Johnson, B., Scher, H. I., Siegel, B. A., Cheng, E. Y., … & Shankar, L. (2005). Progress and promise of FDG-PET imaging for cancer patient management and oncologic drug development. *Clinical Cancer Research, 11*(8), 2785–808.

Meisamy, S., Bolan, P. J., Baker, E. H., Robin, L., Bliss, M. S., Evin, G., … & Michael, G. (2004). Neoadjuvant chemotherapy of locally advanced breast cancer: predicting response with in vivo 1H MR spectroscopy – A pilot study at 4 T. *Radiology, 233*(2), 424–431.

Molina, R., Banez-Coronel, M., Gutierrez, R., Rodríguez-Gonzalez, A., Olmeda, D., Megías, D., & Lacal, J. C. (2004). Choline kinase activation is a critical requirement for the proliferation of primary human mammary epithelial cells and breast tumor progression. *Cancer Research, 64*(18), 6732–6739.

Moller-Hartmann, W., Herminghaus, S., Krings, T., Marquardt, G., Lanfermann, H., Pilatus, U., & Zanella, F. E. (2002). Clinical application of proton magnetic resonance spectroscopy in the diagnosis of intracranial mass lesions. *Neuroradiology, 44*(5), 371–381.

Zhang, C. X., Pan, M. X., Li, B., Wang, L., Mo, X. F., Chen, Y. M. … Ho, S. C. (2013). Choline and betaine intake is inversely associated with breast cancer risk: A two-stage case-control study in China. *Cancer Science, 104*(2), 250–258.